RGNZ/MGPB

Geodynamic and Paragenetic Evolution of the Jbel Houanite Mineralization (Sb-Au; Pb-Zn) Eastern High Atlas of Morocco

Rudarsko-geološko-naftni zbornik
(The Mining-Geology-Petroleum Engineering Bulletin)
DOI: 10.17794/rgn.2026.2.7

Original scientific paper

Jaouad Choukrad[1]* ✉, Abdelkhiar Ait ali[1] ✉, Mohammed Charroud[1] ✉, Nacir El moutaouakkil[2] ✉, Boubker Boukili[2] ✉, Amine Talih[3] ✉

[1] *LaRSI, Science and Engineering Research Laboratory, Faculty of Sciences and Technics, Sidi Mohamed Ben Abdellah University, BP 2202, Fez, Morocco.*

[2] *Geoscience, Water and Environment Laboratory, Faculty of Sciences Rabat, Mohammed V University in Rabat, 4 Avenue Ibn Battouta, B.P. 1014 RP, Rabat, Morocco.*

[3] *Geo-Biodiversity and Natural Patrimony Laboratory (GEOBIO), Geophysics, Natural Patrimony and Green Chemistry Research Center (GEOPAC), Department of Geology and Remote Sensing, Scientific Institute, Mohammed V University, Avenue Ibn Battouta, P.B. 703, 10106 Rabat-Agdal, Morocco.*

Abstract

The district of Jbel Houanite is an important metallogenic province rich in polymetallic mineralization (Sb-Au-Pb-Zn-Ba-Fe-Cu) located in the northern part of the Eastern High Atlas of Morocco, along the North High Atlasic Fault. The earliest identified mineralization corresponds to quartz veins rich in antimony and gold hosted in the Paleozoic formations, while the later mineralization corresponds to Pb-Zn deposits hosted in the Liassic limestones. Geological reconnaissance and mineral exploration work in the Jbel Houanite region determined the presence of antimony mineralization in the form of Stibnite (Sb_2S_3) and Bindheimite ($Pb_2Sb_2O_6(O,OH)$), while the lead mineralization in the sedimentary cover consists of galena (PbS) and cerussite ($PbCO_3$). The lead anomalies are intimately linked to the presence of antimony, and this mineralization is the result of hydrothermal remobilization during the Atlas phases, which reactivated the basement faults, facilitating the establishment of lead mineralization in a Mississippi Valley Type (MVT) system. Petrographic and geochemical investigations of mineral parageneses allowed us to establish temporal relationships between mineralization events: the primary Sb-Au mineralization is linked to late Hercynian extensional tectonics, while the Pb-Zn mineralization is related to early Atlas compressional phases. This sequential evolution highlights a complex polyphase tectono-metallogenic history controlling ore deposition. These findings contribute to a better understanding of the genetic models of Sb-Au-Pb-Zn mineralization in the High Eastern Atlas and demonstrate the crucial role of tectonic inheritance and structural reactivation in ore formation and localization.

Keywords:
Antimony, lead, paragenetic evolution, Paleozoic basement, Meso-Cenozoic cover, Eastern High Atlas, Morocco

1. Introduction

The Eastern High Atlas of Morocco is an intracontinental chain that was formed during the Mesozoic and Cenozoic phases (**Mattauer et al., 1977; Laville et al., 2004; Choukrad, 2022**). This evolution is reflected in the development of pull-apart basins controlled by a network of major faults inherited from the Precambrian and Hercynian tectonic cycles. In this context, the Jbel Houanite mining district is located at the intersection of the North High Atlasic Fault and constitutes a pivotal zone between the Paleozoic structural domain of the Tamlelt inlier and the High Atlasic domain (see **Figure 1a**) (**e.g. Jacobshagen et al., 2005; Nouayti et al., 2023; Chellai et al., 2024**).

The Jbel Houanite region is distinguished by polymetallic mineralization that occurs in two distinct episodes: antimony and gold mineralization (see **Figure 1b**), of Hercynian age, and lead-zinc mineralization, linked to the Atlas orogeny. The former is located along NW-SE and NE-SW oriented fractures, while the latter develops preferentially along the E-W fracture systems intersecting the carbonate platform of the Lower and Middle Lias.

The Paleozoic Tamlelt formations begin with a Neoproterozoic and Cambrian carbonate platform composed of limestones and dolomites. The Cambrian period, marked by black or green pelites with sandstone and quartzitic intercalations, reflects a gradual deepening of the basin (**El Kochri, 1996; Houari, 2003; Houari & Hoepffner, 2003; El Hakour, 2005; Talih et al., 2022**).

* Corresponding author: Jaouad Choukrad
e-mail address: jaouad.choukrad@usmba.ac.ma
Received: 29 May 2025. Accepted: 2 October 2025.
Available online: 13 March 2026

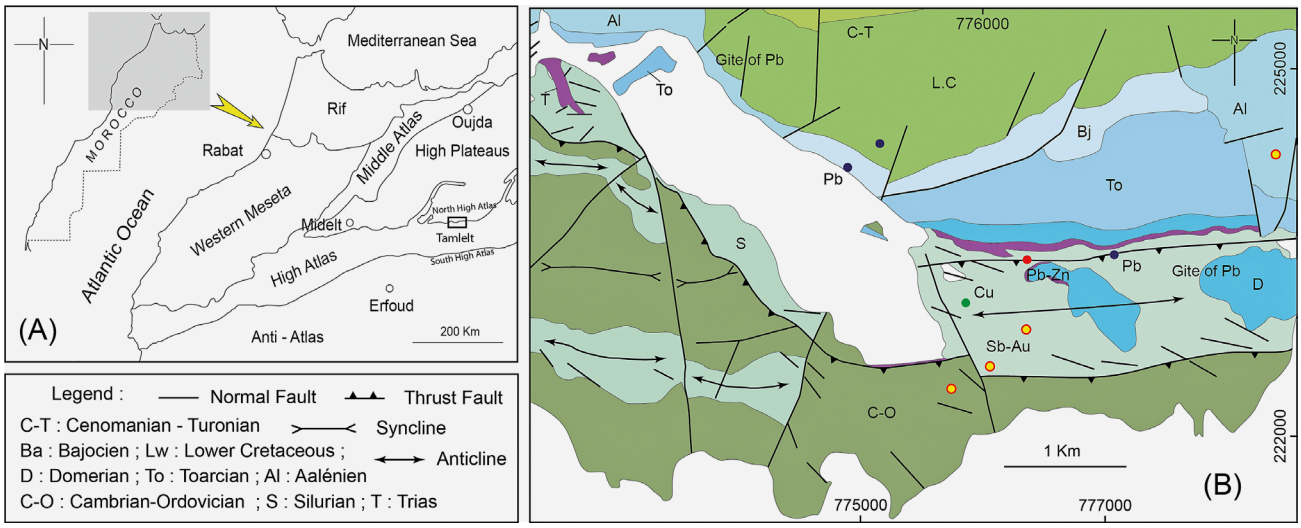

Figure 1. (a) Location of the study area district (b) geological map of Houanite District.

The Ordovician is defined by alternations of sandstone, clayey or silty schist, and quartzites, while the Silurian is represented by silty or clayey pelites (see **Figure 1b**).

The Mesozoic and Cenozoic cover is the result of a negative tectonic inversion initiated in the Triassic and continued during the Jurassic and Cretaceous periods, which led to the formation of sedimentary basins (see **Figure 1b**). The Triassic is characterized by coarse arkoses, conglomerates and sandstones of detrital origin. The Lias, particularly the Sinemurian (see **Figure 1b**), is represented by massive dolomites and limestones reflecting the development of a typical Atlasic carbonate platform (**Charroud et al., 1996; Bezar et al., 1998; Charroud, 2002; Blomeier & Reijmer, 2002; Verwer et al., 2009; Merino-Tomé et al., 2012**). This deposition is followed, between the Pliensbachian and Toarcian periods, by successions of limestone and marl, indicating tectonic activity and the dislocation of the platform (**El Kochri & Chorowicz, 1996; Laville et al., 2004; Choukrad et al., 2024**). The Middle Jurassic begins with Aalenian and Bajocian limestones associated with a reef environment, topped by Bathonian detrital formations (**Kaoukaya et al., 2001; Adil et al., 2004; Choukrad et al., 2022**). The Lower Cretaceous is represented by detrital formations (red sandstones, lacustrine carbonates) dated to the Upper Aptian-Baremian (**El Kochri & Chorowicz, 1988; Haddoumi et al., 1998; Charrière et al., 2005; Haddoumi et al., 2008**). The infra-Cenomanian and Cenomanian levels indicate a detrital-evaporitic environment of sandstone, clay and gypsum, followed by Turonian carbonate deposits.

This study aims to characterize the paragenetic evolution of Sb-Au-Pb-Zn mineralization in the Jbel Houanite region by highlighting the spatio-temporal relationships between the antimony-bearing mineralization of the Hercynian basement and the lead-zinc mineralization hosted in the Mesozoic cover. This analysis is based on a multidisciplinary approach that integrates geological mapping, structural analysis, petrographic studies, and geochemical data.

Despite the significant metallogenic potential of the Eastern High Atlas particularly in polymetallic systems (Sb, Au, Pb, Zn, Fe, Ba, Cu) antimony mineralization in this region remains poorly documented and largely underrepresented in scientific literature. Previous studies have primarily focused on Pb-Zn deposits hosted in the Mesozoic cover (**Adil et al., 2004; Verhaert et al., 2017; Choukrad et al., 2023**), while Sb-Au occurrences in the Paleozoic basement, particularly those associated with shear zones, have received little attention. However, comparable Sb-Au mineralizations located along major crustal structures are well known in other orogenic settings, such as the Massif Central (France) and the Bohemian Massif (Central Europe), where they are typically associated with late hydrothermal fluid circulation controlled by major tectonic structures (**Marcoux & Bril, 1986; Bril et al., 1991; Ashley & Craw, 2004; Craw et al., 2004; Faure et al., 2005**).

In this context, the Jbel Houanite District represents a valuable case study for investigating the genetic links between successive mineralization events, spanning from the Paleozoic Hercynian orogeny to the Cenozoic Atlas orogenic phases.

By comparing the Jbel Houanite system to other Sb-bearing provinces in accretionary orogens, this research provides new insight into the role of inherited structures in controlling polyphase metallogenic systems. It also offers a refined paragenetic framework and temporal constraints that may be applied to other poorly known or unexplored Sb-Au-Pb-Zn occurrences in the High Atlas and analogous geodynamic settings.

2. Methods

In order to identify and characterize the geological and mineralogical aspects, as well as to define the para-

genetic evolution and the modes of mineralization in the region of El Houanite (Eastern High Atlas of Morocco), an integrated methodological approach was adopted, combining field approaches, petrographic, mineralogical and geochemical analyses.

➢ Fieldwork and Geological Mapping

A series of fieldwork campaigns was carried out in order to identify the geological strata, in particular the Paleozoic formations of the schist quartzitic basement and their Meso-Cenozoic cover with predominantly carbonate (limestone and dolomite). The study focused on the geological units containing the Sb and Pb-Zn mineralized showings.

Detailed geological sections and logs were drawn along profiles crossing the mineralized structures. These data were integrated into a geographic information system using ArcGIS 10.8 software to spatialize mineralization in relation to host structures.

➢ Sampling

Twelve representative samples were collected in an area bounded between the coordinates 32°33'58.4"N; 02°27'39.56"W and 32°34'31.27"N; 02°26'23.39"W. These samples cover both the Paleozoic basement (schist and quartzite formations) and the Mesozoic and Cenozoic cover (carbonate formations). Polished thin sections were prepared from selected samples for SEM examination. Prior to SEM analysis, the sections were coated with a thin carbon film using a vacuum carbon coater to ensure electrical conductivity and to improve imaging and EDX signal quality. The carbon coating is necessary to avoid charge accumulation on non-conductive phases and may appear in EDX spectra as an artifact; this was taken into account during data interpretation.

The samples were also examined with the JSM-IT100 Scanning Electron Microscope (SEM), equipped with an Energy Dispersive X-ray (EDX) analysis system semi-quantitative chemical analysis.

The EDX analyses were performed in high-vacuum mode, with an accelerating voltage of 15–20 kV and a working distance of ~10 mm. Elemental mapping and spot analyses were conducted on specific mineral phases to identify their chemical composition and textural relationships.

➢ Mineralogical Analyses (XRD)

The major minerals were identified by X-ray diffraction (XRD), carried out at the laboratory of the University of Fez using a Philips PANalytical X'Pert Pro diffractometer (Cu-Kα radiation, λ = 1.5406 Å, voltage 40 kV, intensity 40 mA). The analyses were performed at room temperature on powders obtained after fine grinding of the samples at a 50 μm mesh sieve, in order to minimize the effects of texture and preferential orientation. Data processing was carried out via the X'Pert Data Collector software.

➢ Geochemical analyses (XRF and ICP-MS)

The twelve collected samples were also the subjected to geochemical analyses to quantify major, minor and trace elements. The major elements were determined by wavelength dispersive X-ray fluorescence (XRF, Axios model), according to the standardized PROT ELE03-v01 protocol, after drying and conditioning the samples in granular form.

We followed the NI 43-101 standards for mining work using quality control procedures on geochemical analyses that correspond to the use of one sample doubling for every 10 samples and certified blank samples to ensure the reliability of the results and geochemical analyses.

Trace elements were analyzed by inductively coupled plasma mass spectrometry (ICP-MS) using an Ultima 2 - Jobin Yvon spectrometer, according to the NF EN ISO 11885. The results of these analyses are summarized in **Table 1**.

➢ Structural data treatment

We have processed the different tectonic structural measurements using the "Win-Tensor" software developed by the structural geologist Dr. Damien Delvaux (**Delvaux & Sperner, 2003**), this program is widely adopted and redundant, having already been used in scientific publications worldwide for processing tectonic and structural data results.

➢ Objective of the integrated analytical approach

The combination of these different analytical techniques (mapping, optical and electron microscopy, X-ray diffraction, X-ray fluorescence, ICP-MS) has made it possible to establish a clear link between the types of mineralization and their geological context. This cross-referencing of the data has contributed to the reconstruction of the paragenetic evolution of the antimony mineralization of the basement and the lead-bearing mineralization of the cover.

3. Results

Houanite District is a polymetallic province known for various types of mineralization; the location of the mineralized bodies of the Houanite District and their hosted rock has allowed us to indicate the presence of stages of mineralization with a paragenetic relationship between them. The first ore bodies associated with N120 and N40 quartz veins and they are composed by antimony and gold hosted in the Paleozoic formations, while the second one is hosted in the Liassic limestones following the Atlasic fracturing and the karstification area.

3.1. The Paleozoic inlier ore deposit

The antimony mineralization (Sb) is mainly located along major fracture and fault systems affecting the Paleo-

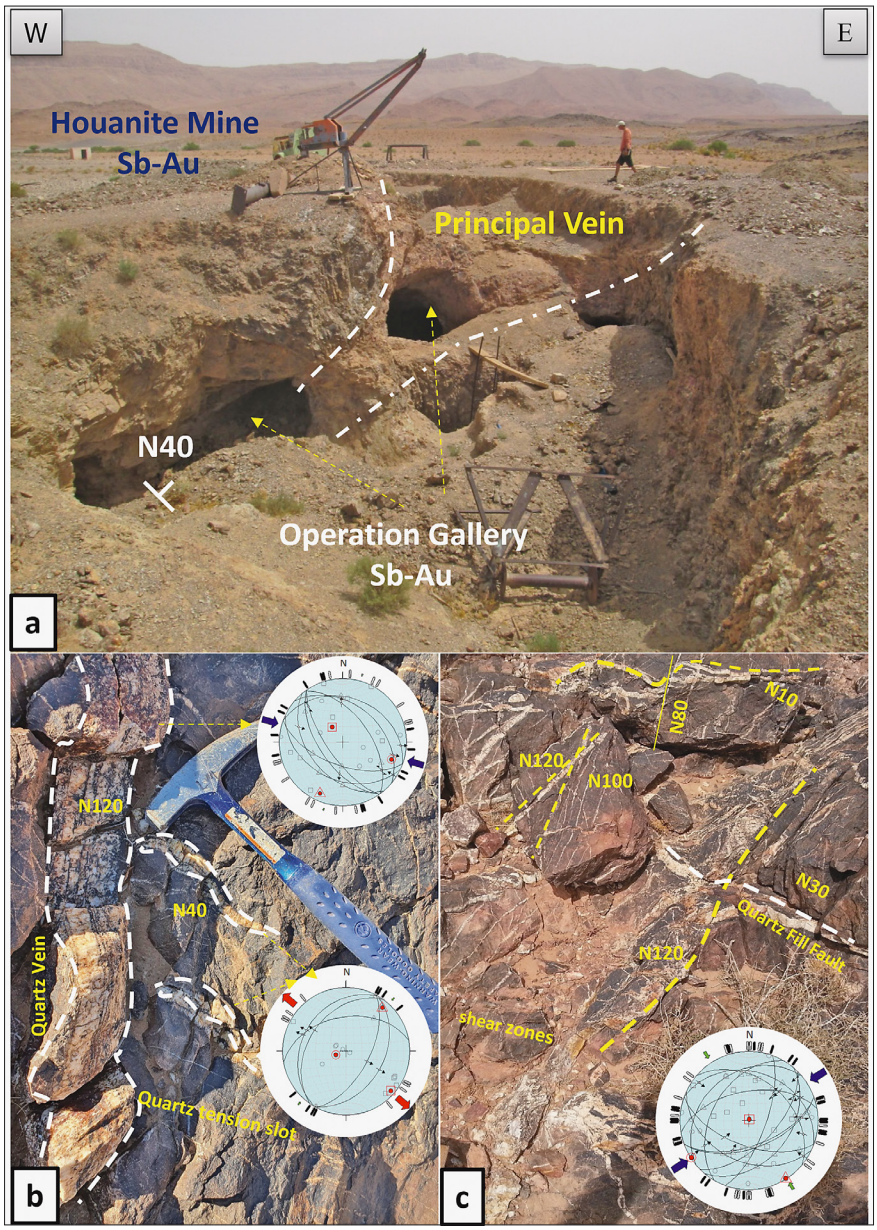

Figure 2. Detailed photos of the Houanite Au-Sb mining sector (a) the Houanite mine zone, (b) showing mineralization associated with quartz veins and stereographic representation of structural measurements (c) Deformation shear zone with the different generation of quartz rich in Sb-Au- and stereographic representation of structural measurements.

zoic basement (see **Figure 2a**). These structures have a dominant orientation between NW-SE and NE-SW, suggesting a polyphase tectonic heritage (**Ashley & Craw, 2004; Azza et al., 2019; Choukrad, 2022**). The structural ground analysis, coupled with the study of the spatial distribution of the orebodies, indicates that the mineralization is controlled by shear zones and deformation corridors associated with these large faults (see **Figure 2c**).

Three main episodes of deformation have been identified:

➢ Episode D_1: NW–SE Extension:

The first tectonic episode is characterized by an extensional regime-oriented NW–SE. This phase led to the formation of normal faults with apparent displacement along a N40° direction (approximately NE–SW) (see **Figure 2b**). These faults are commonly filled with quartz and, in some areas, show the presence of stibnite and gold-bearing mineralized bands.

➢ Episode D_2: NE–SW Compression:

The second episode corresponds to a compressive regime-oriented NE–SW, marked by reverse faults, open to tight folds, and ductile shear zones. Some of the earlier extensional structures were reactivated during this phase, displaying transpressive kinematics (see **Figure 2b).**

➢ Episode D_3: NW–SE Compression

A third compressive episode, oriented NW–SE, is also recognized. It is expressed by late-stage deformation features such as fault intersections and folding, which locally overprint earlier structures (see **Figure 2c**). This phase contributed to the development of fine-scale fracturing in previously deformed zones.

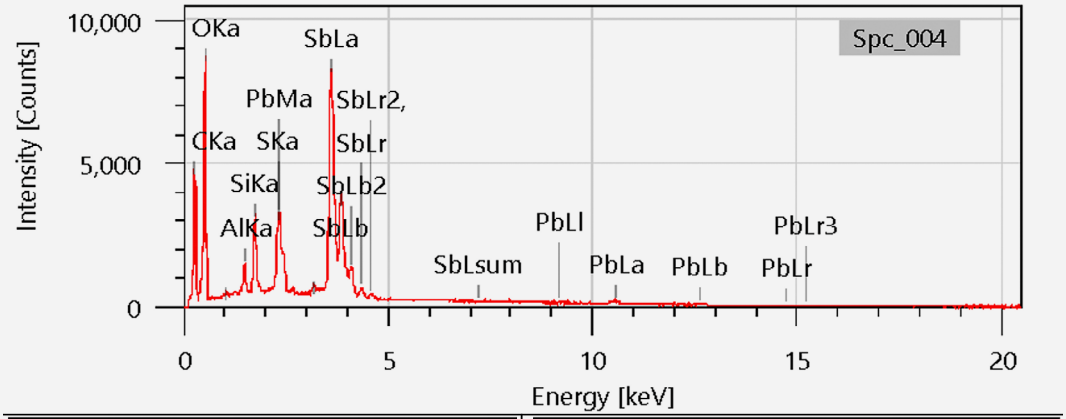

Element	Line	Mass%	Atom%
C	K	27.00±0.06	54.14±0.13
O	K	23.57±0.13	35.48±0.19
Si	K	0.43±0.03	0.37±0.02
S	K	0.79±0.03	0.59±0.02
Sb	L	46.75±0.27	9.25±0.05
Total		100.00	100.00
Spc_004			Fitting ratio 0.0440

Stibnite (Sb2S3) possibly Valentinite / Senarmontite (Sb_2O3)

Element	Line	Mass%	Atom%
C	K	27.00±0.06	54.14±0.13
O	K	23.57±0.13	35.48±0.19
S	K	0.79±0.03	0.59±0.02
Sb	L	46.75±0.27	9.25±0.05
Pb	M	1.47±0.010	1.17±0.01
Total		100.00	100.00
Spc_004			Fitting ratio 0.0440

Bindheimite ($Pb_2Sb_2O_6(O, OH)$) possibly Valentinite / Senarmontite (Sb_2O3)

Figure 3. Semi-quantitative compositions of Sb-bearing Paleozoic inlier ore samples from Houanite District (targeted sample)

The observed structural context suggests that the mineralizing episodes were multi-phased, with initial mineralization mainly related to the extensive D_1 phase, followed by reactivation and concentration events controlled by the D_2 and D_3 compressive phases. This polyphase tectonic control underscores the importance of shear corridors as major hosts of stibnite and gold deposits in this region.

The research and exploitation work by gallery, well, and open pit revealed the presence of polymetallic deposits (Sb-Au-As) in the basement (see **Figure 2a**). The general structures measured led to a typical dexterous shear zone. This zone is considered a transformation zone in Paleozoic times (**Piqué & Michard, 1989; Dill, 1998; Houari & Hoepffner, 2003; Azza et al., 2019; Jaouad et al., 2024**). The mineralization observed in the field is hosted in quartz veins intersecting middle Cambrian sandstone and quartzite.

In the field the folding belt ENE - WSW with regional development of the vertical axial plane cleavage. This deformation shows ductile faults associated with vertical foliation with mineralization of stibnite and chalcopyrite. The Sb-Au mineralization is emplaced in locally irregular 40-50 cm quartz veins (stockwork) (see **Figure 2c**). Quartz veins are observed in some places explaining the mode of emplacement of this mineralization in a shear-zone type shear zone.

Petrographic observation by optical microscopy of the samples indicated gold mineralization showing gold pipettes injected into the sub-automorphic quartz of the microgranites. While stibnite is disseminated in quartz and plagioclase, feldspars with chlorite with a very large portion in the rock. Thus, we can conclude that the paragenetic ores of the Paleozoic basement are composed of Sb-Pb (see **Figure 3**).

Scanning Electron Microscope (SEM) analysis combined with Energy-Dispersive X-ray Spectroscopy (EDS) was conducted on samples collected from mineralized quartz veins within the Paleozoic basement of the Houanite District. Multiple mineral assemblages were identified based on their chemical signatures. EDS spectra reveal the presence of antimony in association with lead, sulfur, oxygen, and silica (**Choukrad et al., 2022; Rajeshkumar et al., 2024; Sun et al., 2024**).

The EDS data display variable concentrations of sulfur and lead, reflecting local chemical heterogeneity within the mineralized zones. Complementary (XRD) analyses performed on the same samples allowed for the definitive identification of Stibnite (Sb_2S_3) and Bindheimite ($Pb_2Sb_2O_6(O,OH)$) (see **Figure 4a** & **d**). These mineral phases were further corroborated by ore microscopy observations, confirming their presence and textural relationships within the quartz veins.

The EDS spectra presented in **Figure 3** were initially interpreted as evidence of the presence of Stibine (Sb_2S_3) and Bindheimite. However, a reevaluation of the chemical data suggests the presence of an antimony oxide. Valentinite (Sb_2O_3), Secondary alteration product com-

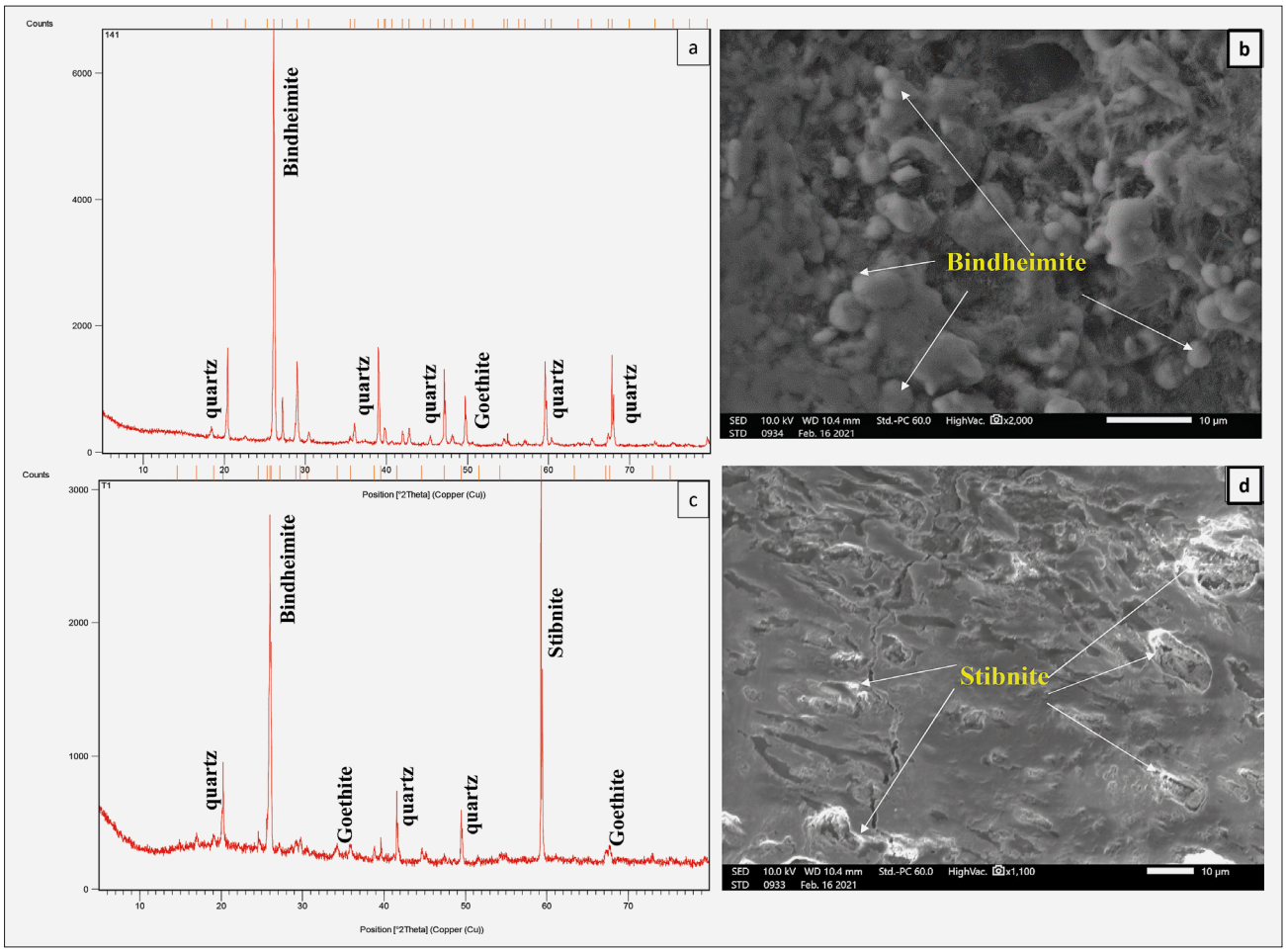

Figure 4. X-ray diffraction analysis of antimony samples from the Houanite basement; (a) X-Ray Diffraction, (b) Bindheimite scale microscope observation, (c): results of X-Ray Diffraction (d): stibnite scale microscope observation.

monly observed in oxidized zones of antimony deposits, was thus considered as a probable phase. In order to validate this hypothesis, additional X-ray diffraction (XRD) analyses were performed (see **Figure 4**). However, the obtained diffractograms do not confirm the presence of either Valentinite or Senarmontite, these two polymorphs share an identical chemical formula (Sb_2O_3). This absence of distinctive crystalline signals could indicate that the antimony oxide present is either amorphous or weakly crystallized, making its identification by XRD inconclusive.

3.2. The Mesozoic and Cenozoic cover ore deposit

The mineralization is embedded in the Mesozoic and Cenozoic cover of Jbel Houanite following faults of major directions varying from E-W to NW-SE structurally parallel to the North High Atlasic Accident (see **Figure 5, a** & **d**) and also to the Hercynian inheritance faults. The mineralization is mostly found in the limestones and dolomites of the Domerian and Toarcian, which are Mesozoic and Cenozoic formations (see **Figure 5b, c** & **e**). The mineralized structures are hosted in the fault N90 and follow the karstification area. The mineralization indicates the presence of Pb-Zn-Ba-Calcite (**Munoz & Moëlo, 1982; Leach et al., 2005; Wei et al., 2020; Lafforgue et al., 2021; Choukrad et al., 2022; Ait Ali et al., 2024; Choukrad et al., 2024; Sun et al., 2024; Ait Ali et al., 2025**).

During the Jurassic, the Mesozoic sedimentary cover of the region was affected by a major tectono-sedimentary phase attributed to the Atlas orogeny. Field observations indicate an extensive tectonic regime, evidenced by a dense network of normal faults and sub-vertical dislocations (see **Figure 5a**), oriented mainly NE–SW and NW–SE. These structures are associated with the development of karstic cavities and brecciated zones, locally filled with carbonate cement and sulfide mineralization.

Structural data reveal that E–W trending faults intersect and link the two main extensional systems. These faults show features suggesting their possible role as transfer zones or relay structures (see **Figure 5d**). The mineralized bodies are mainly hosted within fractured and karstified carbonate formations, spatially associated with these structural features.

The geometric relationships observed between mineralized zones, karst features, and fault systems suggest a

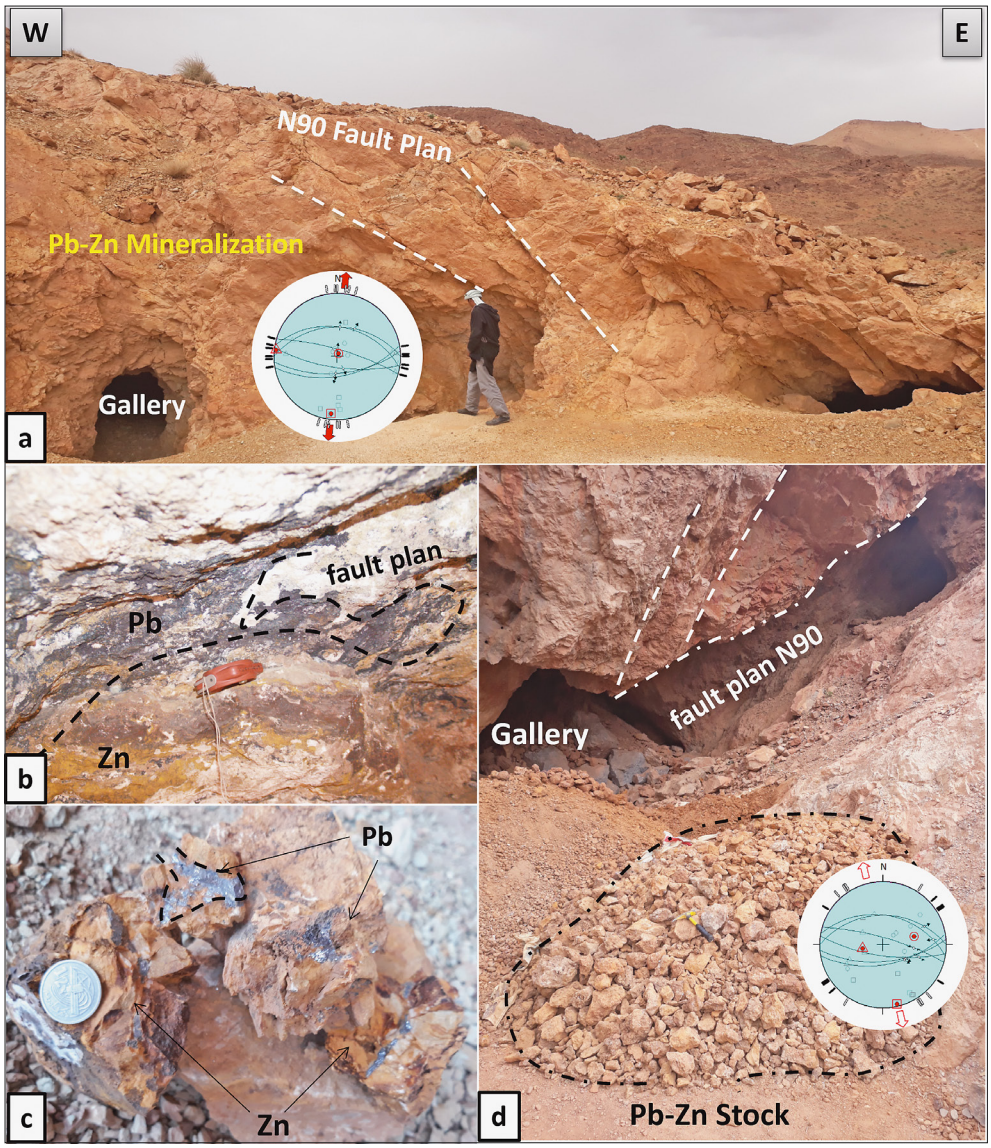

Figure 5. Pb-Zn mineralization of the El Houanite District (a) Pb-Zn- mine and mining gallery along the N90 normal fault with stereographic representation of structural measurements along the N90 fault. (b & c) samples of high-grade Pb-Zn mineralization from the Mezosoic canopy (d) Mined Pb-Zn suivant la faille normale N90 with stereographic representation of structural measurements.

strong structural control on the spatial distribution of the Pb-Zn mineralization during this post-Liassic phase. Further implications regarding fluid migration, mineralization processes, and tectono-sedimentary interactions are discussed in the Discussion section.

Scanning Electron Microscope (SEM) analysis, coupled with Energy Dispersive X-ray Spectroscopy (EDS), performed on samples collected from the lead-zinc mineralized zones within the Mesozoic cover of the Jbel Houanite District, reveals the presence of several mineral assemblages, identified based on spectral peaks and elemental proportions. Lead is detected in association with sulfur, carbon, and oxygen, corresponding respectively to sulfide (galena, PbS) and carbonate (cerussite, $PbCO_3$) phases. These minerals are frequently associated with smithsonite ($ZnCO_3$).

It is important to note that the silica detected in some EDS spectra does not indicate the presence of lead silicate minerals. It most likely results from adjacent quartz grains included in the analyzed area, as the EDS beam interaction volume is large enough to encompass multiple mineral phases simultaneously. Therefore, the co-occurrence of Si and Pb peaks should not be interpreted as a direct chemical or mineralogical association.

The simultaneous detection of Pb and Sb peaks in certain samples (see **Figure 6**) may indicate either the coexistence of distinct Sb and Pb-bearing minerals within the same analyzed area, or partial remobilization of antimony into the lead-zinc mineralization system. However, these interpretations should be approached with caution, as EDS provides only bulk chemical data, and not direct mineralogical identification.

These interpretations were therefore cross-checked and confirmed by X-ray Diffraction (XRD) analyses, which allowed for the definitive identification of mineral phases such as galena and cerussite. The correlation between (EDS) and (XRD) data validates the presence of these mineral assemblages and reinforces their geological significance.

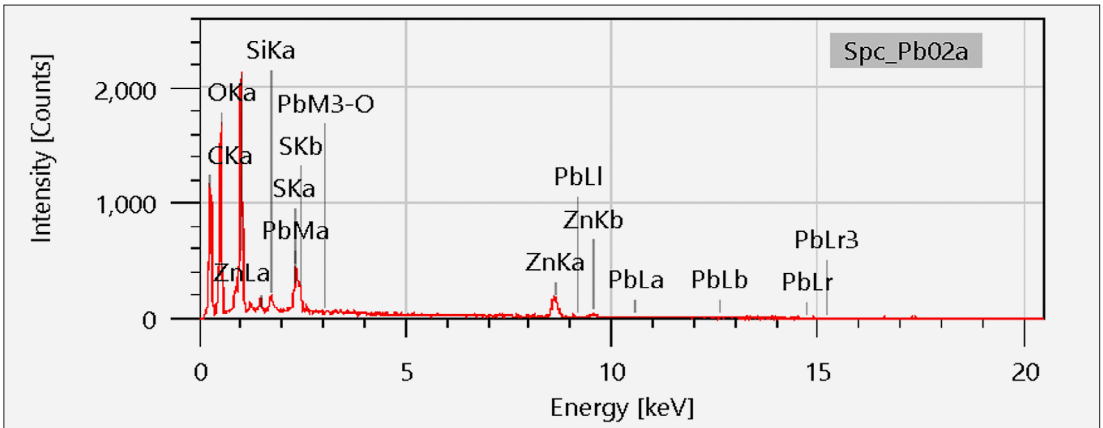

Element	Line	Mass%	Atom%
C	K	6.68±0.06	25.59±0.24
O	K	19.08±0.21	54.91±0.59
Al	K	0.41±0.04	0.70±0.06
Zn	K	4.95±0.25	3.49±0.17
Pb	M	68.88±0.44	15.31±0.10
Total		100.00	100.00
Spc_002			Fitting ratio 0.0624

Cerussite ($PbCO_3$) + Smithsonite ($ZnCO_3$)

Element	Line	Mass%	Atom%
C	K	6.50±0.05	27.63±0.21
O	K	14.59±0.14	46.55±0.45
Al	K	0.45±0.03	0.85±0.05
S	K	4.19±0.007	6.67±0.11
Pb	M	74.26±0.37	18.29±0.09
Total		100.00	100.00
Spc_002			Fitting ratio 0.0594

Galena (PbS) + Cerussite ($PbCO_3$)

Figure 6. SEM analyse with the semi-quantitative compositions of Pb-bearing Mesozoic cover ore samples from the Houanite District (targeted sample)

Observation of polished blades taken from mineralized structures in the Jbel Houanite District reveals the presence of several lead mineral phases, including galena (PbS) (see **Figure 7a** & **b**), anglesite ($PbSO_4$) and cerussite ($PbCO_3$) (see **Figure 7, c** & **d**). Other indices testify to the hydrothermal activity and its remobilization from the base up to the cover, which are arsenopyrite and the iron oxides. Moreover, the galena is surrounded by the iron oxide represented by hematite, indicating that the initial mineralization was followed by the alteration in an oxidizing environment.

The microscopic observation of twelve samples taken in the mineralized Mesozoic cover of Jbel Houanite has revealed a complex and polyphase paragenesis. Lead mineralization is mainly represented by Galena (PbS) (**Figure 7a** & **b**), often accompanied by its supergene alteration products (see **Figure 7c** & **d**). The occurrence of cerussite is consistent with the oxidation of primary galena in the presence of sulphate- and carbonate-rich fluids, under conditions typical of meteoric alteration environments. The coexistence of galena and cerussite suggests progressive oxidation under variable redox and pH conditions, characteristic of the supergene domain (**Chapman et al., 2022; Ece & Ercan, 2024; Choukrad et al., 2024**).

In contrast, the presence of iron oxides and arsenopyrite indicates the involvement of higher-temperature hydrothermal processes, possibly linked to earlier mineralizing phases. These minerals are generally associated with deeper fluid circulation during tectono-metamorphic evolution (**Oh et al., 2004 ; Iancu et al., 2005; Caddick & Thompson, 2008**). The observed vertical mineralization patterns, extending from the Paleozoic basement to the overlying formations, suggest that mineralizing fluids may have migrated upward along fracture systems or fault zones.

It is particularly noteworthy that Galena is frequently bordered or enclosed by iron oxides. This arrangement reflects post-mineralization hydrothermal alteration under oxidizing conditions. This mineralogical overprint indicates that after the deposition of the galena, a late episode of circulation of oxidizing fluids induced a partial transformation of the primary sulphides.

The entire mineralogical assemblage and the observed textural relationships support a mineralization model with two main phases: an early phase of hydrothermal sulphide deposition, followed by an episode of supergene alteration in an oxidative context. This evolution testifies to the interaction between deep hydrothermal processes and surface meteoric alteration phenomena, controlling the distribution of mineralization and the mobility of metals in the Jbel Houanite District.

3.3. Geochemical study

Geochemical analysis of twelve samples of the mineralized basement and cover structures shows significant concentrations of antimony and lead, according to **Table 1** noting that lead concentrations are closely related to that of antimony.

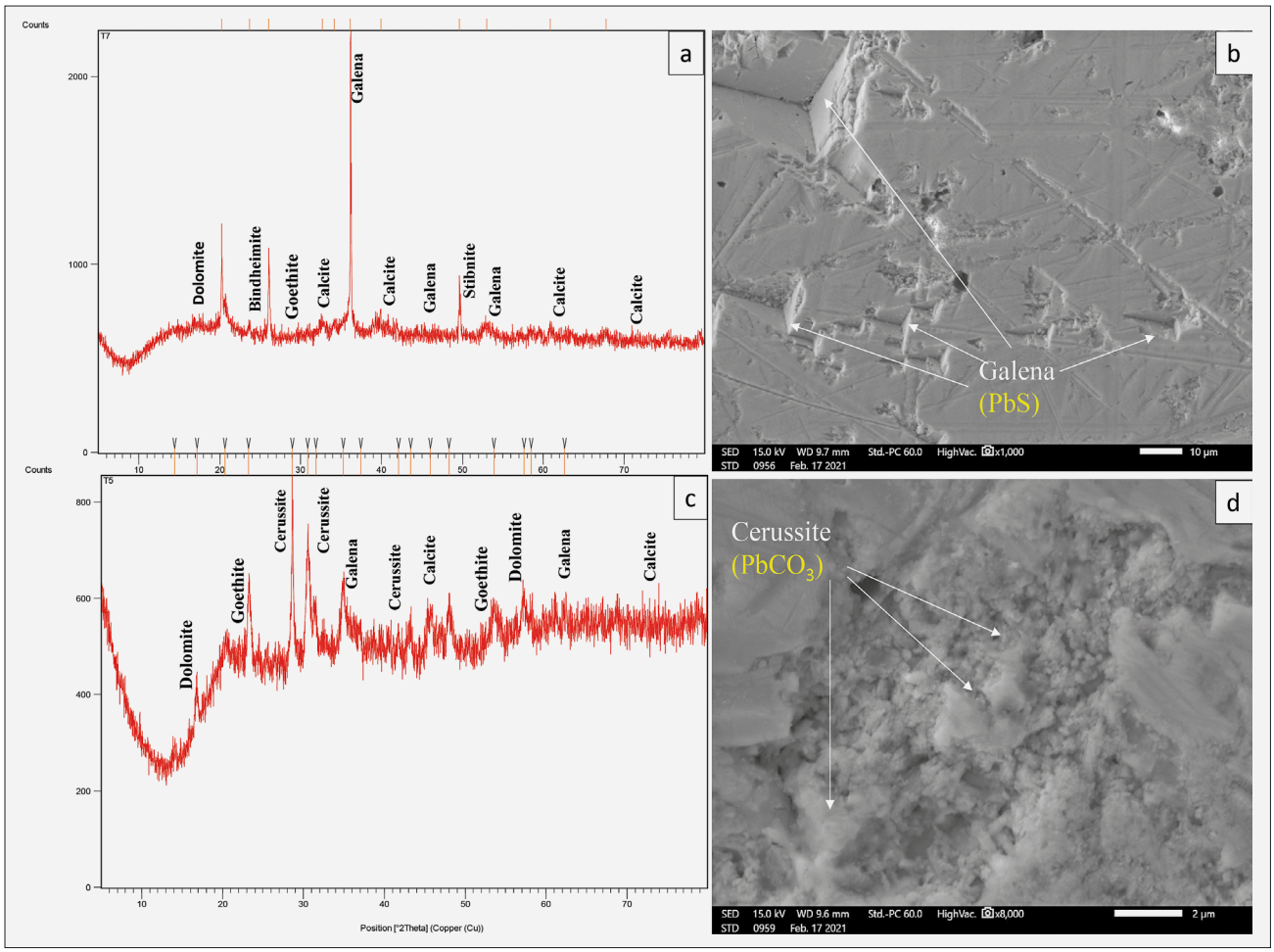

Figure 7. X-ray diffraction analysis of the Mesozoic cover ore deposit in the El Houanite District; (a) X-Ray Diffraction, (b) Galena scale microscope observation , (c): X-ray diffraction results (d): Cerussite scale microscope observation.

Table 1. Geochemical analysis by ICP-MS samples of Jbel Houanite

	Au (ppm)	Ag (ppm)	As (ppm)	Ba (ppm)	Cr (ppm)	Cu ppm)	Fe (%)	Pb (ppm)	S (%)	Sb (ppm)	Sn (ppm)	Te (ppm)	Ti (%)	Zn (ppm)
JH003	0.005	0.11	1.6	1140	1	16.6	23.7	4.6	0.24	2.13	0.2	0.07	0.005	40290
JH004	0.005	0.02	0.4	1800	2	29.2	0.35	5200	0.12	70000	0.2	-0.05	0.005	2
JH007	0.005	0.06	5	420	8	41.2	10.25	1450	0.01	2800	0.2	-0.05	0.005	32451
JH008	0.005	0.32	7.6	5250	7	10.1	37.1	2602	0.13	50000	0.2	-0.05	0.017	27
JH014	0.005	0.14	6.9	170	41	27.9	1.68	22100	0.01	56000	0.2	-0.05	0.062	58
JH017	0.005	0.07	2.9	20	34	13.1	0.77	12500	0.01	210000	0.2	-0.05	0.005	4
JH026	12.45	0.87	54.8	530	60	38.3	3.5	57200	0.12	220000	0.9	0.13	0.12	206
JH028	13.55	0.91	57.4	530	47	37.4	8.79	54300	0.33	390000	0.3	0.19	0.038	199
JH029	121	2.61	39.4	130	34	75	0.82	18400	0.05	400000	0.2	0.18	0.018	103
JH030	2.81	0.37	48.6	200	68	31.3	1.9	31300	0.45	450000	0.5	0.08	0.084	1909
JH031	0.156	0.3	102	390	75	30.1	2.32	1480	0.01	2150	1.2	-0.05	0.325	12500
JH032	0.005	0.88	113.5	1260	41	118	1.22	291	0.05	34.1	0.2	0.05	0.005	158

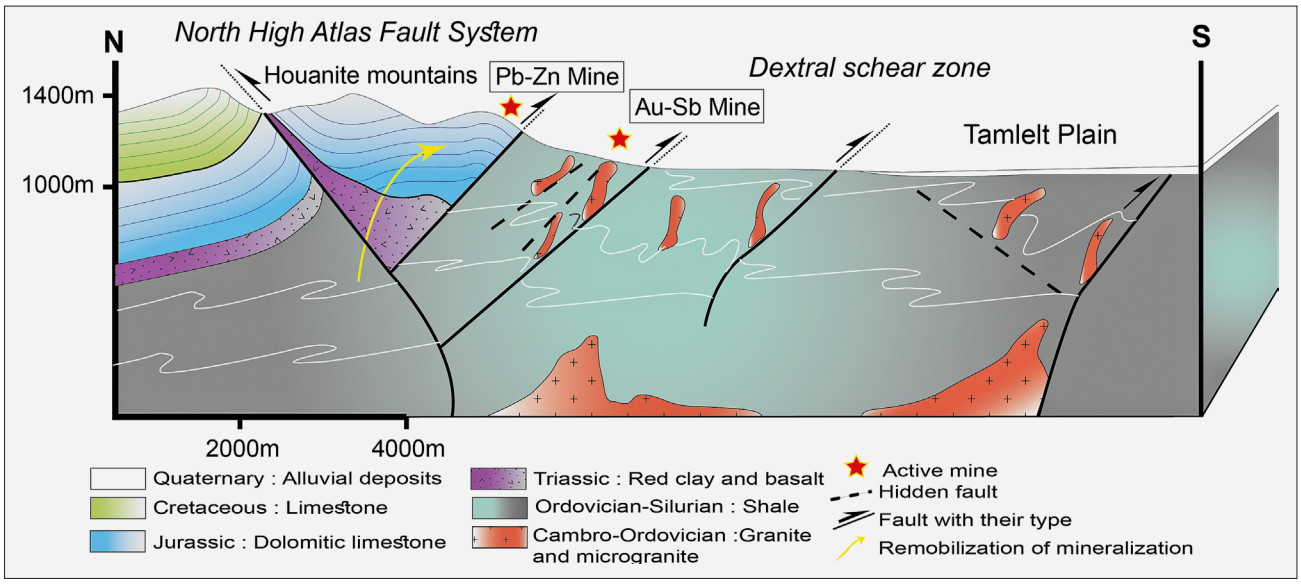

Figure 8. Geological section showing hydrothermal circulations and the passage of Au-Sb and Pb-Zn mineralization from the basement to the cover.

In particular, samples JH026, JH028, JH029 and JH030 show significant grades of Sb, Au, As and Pb (see **Table 1**). It is important to note that samples JH030 and JH031 are from the Meso-Cenozoic cover. The presence of gold provides evidence of paragenetic evolution and migration of mineralization from the basement to the cover, which resulted in the migration of gold and arsenic grains.

The results of the geochemical analyses made it possible to distinguish two sample populations:

- **Group 1**: samples from the Paleozoic basement rich in antimony (up to 45%), As, Au (trace values detected), accompanied by high Fe and S (see **Table 1**).
- **Group 2**: samples from the Mesozoic cover rich in Pb (up to 6%), Zn, Ba (trace values detected) (see **Table 1**).

ICP-MS analyses also revealed anomalous concentrations of trace elements such as Ag, Cu, Cr, Ti in the transition zones between the two types of mineralization, suggesting interactions between hydrothermal systems.

4. Discussion

Based on the various geochemical studies, petrographic and metallogenic observations and macroscopic examination of samples, two types of primary mineralization were determined. The Sb-Au mineralization in the basement related to large "shear zone" shear bands cemented by partially corroded quartz veinlets related to the Hercynian orogeny, and a second type of later Pb-Zn mineralization (see **Figure 8**) hosted in the Meso-Cenozoic cover related to the Atlas orogeny. The structural evolution, marked by successive extensional and compressive events (D_1 to D_3), played a significant role during the deposition of these mineralization types, controlling the fluid flow and ore localization. The D_1 extensional regime appears to have created permeable fault zones that facilitated the initial circulation of hydrothermal fluids and the deposition of stibnite- and gold-bearing mineralization. Subsequent compressive phases (D_2 and D_3) likely reactivated earlier structures, promoting remobilization and local concentration of mineralization within transpressive shear zones and structural traps (**Ashley & Craw, 2004**). This polyphase tectonic evolution highlights the critical role of structural inheritance and reactivation in ore system development (see **Figure 8**).

The mineralization is mainly located along major fractures and faults, with two dominant systems:

- NW-SE to NE-SW system, affecting the Paleozoic basement, hosting the stibnite (Sb_2S_3) bindheimite ($Pb_2Sb_2O_6(O,OH)$), and valentinite (Sb_2O_3) mineralization.
- E-W system, affecting Liasic carbonates, containing galena (PbS), anglesite (PbSO4), cerussite (PbCO3) and smithsonite (ZnCO3) mineralization.

Noting that the Pb, Sb mineralization's are intimately related to each other, while we have not observed a remarkable relationship between the grades of antimony and zinc, nor of lead and zinc, this explains the genetic relationship of the Pb/Sb mineralization's, and gives us a clear idea that these two types of mineralization are the result of a mineralogical evolution that has lasted for a long time (**Chovan et al., 1995; Dill, 1998; Clayton & Spiro, 2000**).

SEM-EDS analyses, combined with X-ray diffraction results, confirm the presence of Stibnite (Sb_2S_3) and Bindheimite ($Pb_2Sb_2O_6(O,OH)$) in the quartz veins. The

variability in lead and sulphur contents observed by EDS reflects local heterogeneity related to alteration processes. The presence of secondary antimony oxides, such as Valentinite and Senarmontite (Sb_2O3), is strongly supported by EDS data; however, it remains hypothetical pending confirmation by XRD. The silica detected by EDS likely corresponds to quartz micro-inclusions captured during analysis, without direct mineralogical association. Finally, the carbon detected in the EDS spectra is attributed to the conductive coating applied to the samples and is not considered a mineral component.

The presence of antimony in the form of Bindheimite ($Pb_2Sb_2O_6(O,OH)$, indicates an advanced stage of oxidation and remobilization of primary lead and antimony sulfides in a supergene environment (**Dill, 1998; Munoz & Moëlo, 1982; Sun et al., 2024**).

The transition towards secondary stibnite (Sb_2S_3) mineralization suggests a transformation under changing physicochemical conditions, particularly a decrease in oxygen activity and an increase in sulphur activity. This process likely involved the reduction of antimony, along with the release of lead and oxygen, possibly associated with a late hydrothermal or diagenetic event (**Dill, 1998; Munoz & Moëlo, 1982**).

The late overprinting of Stibnite (Sb_2S_3) by Bindheimite ($Pb_2Sb_2O_6(O,OH)$ highlights a complex paragenetic sequence (see **Table 2**), controlled by fluctuations in redox potential and geochemical conditions within the system.

The existence of Galena (PbS) and its alteration products reflects progressive oxidation under redox and pH conditions typical of the supergene environment, influenced by meteoric fluids enriched in sulfates and carbonates (**Chapman et al., 2022; Ece & Ercan, 2024**). The occurrence of arsenopyrite and iron oxides suggests an earlier high-temperature hydrothermal phase, likely associated with deep fluid circulation during a tectono-metamorphic event (**Oh et al., 2004; Iancu et al., 2005; Caddick & Thompson, 2008**). The vertical remobilization of mineralizing elements from the Paleozoic basement to upper stratigraphic levels suggests ascendent fluid migration, probably facilitated by fracture or fault systems.

On the basis of the various geochemical studies and petrographic and metallogenic observations and by macroscopic examination of the samples, the mineralization's of the Jbel Houanite District were formed in several successive stages, the first three correspond to the mineralization's deposited at the different phases of the Hercynian orogeny, these are the antimony, copper and arsenic mineralization, after remobilization of the latter in note the establishment of mineralization's at lead and zinc during the phases of the atlas orogeny (see **Figure 9**).

The results obtained through the different analysis methods (geological mapping, petrographic observations, XDR, SEM-EDX, XRF and ICP-MS analyses) have highlighted the lithological diversity, the characteristic mineralogical associations, as well as the paragenetic evolution of the Sb and Pb mineralization's in the Jbel Houanite District.

Observations under the light and electron microscope have identified several distinct mineral associations:

- **Sb-Au mineralization (Paleozoic basement):**
  - Main minerals: stibnite, bindheimite, pyrite, quartz.
  - Textures: fracture filling, vein and veinlet structure, local stibnite zonation, surface antimony oxide alteration.
  - Accompanying mineralogy: sericite, chlorite, sometimes native gold in the microscopic state.
  - The high oxygen content observed in some EDX spectra is likely related to the presence of valentinite and senarmontite (Sb_2O_3), an antimony oxide phase (see **Table 2**), although it was not identified by XRD.
- **Pb-Zn mineralization (Meso-Cenozoic cover):**
  - Main minerals: galena, cerussite, sphalerite, iron oxides, calcite.
  - Secondary minerals: dolomite, barite.
  - Textures: filling of karst cavities, cementation of sub-horizontal fractures, sometimes as a replacement for the host dolomite.

XRD analysis confirmed the predominance of carbonate phases (calcite, dolomite) in the host rock, with clear peaks of Stibnite and Galena in the mineralized samples.

The cross-analysis of textures, mineralogical relationships and structural contexts has made it possible to propose:

- **Phase 1 (Hercynian-Paleozoic):**
  - **Stage I:** The antimony mineralization in the basement, associated with a circulation of hydrothermal fluids along the NW-SE and NE-SW fractures. The environment is reductive, at moderate temperature, with precipitation of Stibnite (Sb_2S_3), quartz, pyrite, and calcite (see **Table 2**).
  - **Stage II:** Corresponds to a continuation of hydrothermal activity with precipitation of stibine (Sb_2S_3), galena (PbS), quartz and calcite, in an environment in transition to slightly oxidizing conditions. The appearance of bindheimite ($Pb_2Sb_2O_6(O,OH)$), valentinite and/or senarmontite (Sb_2O_3) and anglesite (PbSO4) affirms to an early alteration of lead sulphides (see **Table 2**). Although EDS data suggest the presence of antimony oxide, their formation is more likely related to later supergene alteration (phase III).
- **Phase 2 (Atlasic- Meso-Cenozoic):**
  - **Stage III:** It is manifested by the development of secondary antimony oxides, under the effect of oxidizing conditions in a subaerial context. On

Table 2. Paragenetic Sequence and Mineralogical Evolution in the Jbel Houanite District, Eastern High Atlas (Morocco).

MINERALS	STAGE- I	STAGE- II	STAGE- III
Stibnite (Sb_2S_3)	-- -- -- -- -- --	-- -- --	
Valentinite (Sb_2O_3)		-- ----	-- --
Sénarmontite (Sb_2O_3)		-- -- --	-- --
Bindheimite ($Pb_2Sb_2O_6(O,OH)$)		-- -- --	-- --
Gold (Au)	-- -- --	-- --	
Galena (PbS)		-- -- -- -- -- --	
Anglesite ($PbSO_4$)		-- -- --	-- -- -- --
Cerussite ($PbCO_3$)			-- -- -- -- -- --
Smithsonite ($ZnCO_3$)			-- -- --
Quartz (gangue)	-- -- -- -- -- --	-- -- -- --	
Calcite ($CaCO_3$)	-- -- --	-- -- --	-- --
Goethite ($FeO(OH)$)	-- -- --	-- -- --	-- -- -- --

-- -- presence of the mineral during the phase

the other hand, it corresponds to the deposition of lead mineralization in the carbonate cover, via cerussite (PbCO3) and smithsonite (ZnCO3) (see **Table 2**). enriched hydrothermal circulations, transported along the E-W faults. This phase is marked by an active tectono-sedimentary environment, with filling of karst cavities and hydrothermal replacement.

The contact zone between basement and cover locally shows a superposition of the two systems, suggesting a structural reactivation allowing the partial remobilization of the previous mineralization.

5. Conclusions

This study combines geochemical, petrographic, metallogenic, structural, and macroscopic analyses performed on samples from the Jbel Houanite area. The integrated results allowed the identification of antimony mineralization mainly in the form of stibnite (Sb_2S_3) and bindheimite ($Pb_2Sb_2O_6(O,OH)$) within the Paleozoic basement, as well as lead and zinc mineralization, notably galena (PbS) and cerussite ($PbCO_3$), occurring in the Meso-Cenozoic cover (see **Figure 9**).

Structurally, these mineralizations are closely associated with major fault zones and shear bands resulting from a polyphase tectonic evolution marked by the Hercynian and Atlas orogenies. Successive tectonic events alternating between extensional and compressional phases (D_1, D_2, D_3) controlled hydrothermal fluid circulation and ore deposition, with the initial extensional phase promoting fluid flow and mineral precipitation, while later compressional phases contributed to remobilization and local concentration of mineralization within transpressive shear zones and structural traps.

From a geodynamic perspective, the Sb-Pb deposits developed in accretionary orogenic settings, typically hosted in granitic, greenstone, and meta-sedimentary turbidite terrains. Their formation is temporally linked to the late stages of the Hercynian orogeny and the early phases of the Atlas orogeny (see **Figure 9**).

In the light of mineralogical and structural observations, a paragenetic evolution in several stages is proposed, illustrating a variation of the metal assemblies as a function of depth, with an enrichment of antimony in the upper levels.

Gold-bearing stibnite (Sb_2S_3) constitutes the primary phase of mineralization, developed in a hydrothermal context associated with a Hercynian fracture network, in a compressive to transpressive tectonic setting. The establishment of this mineralization is probably controlled by structural release zones, in connection with major discontinuities favorable to the circulation of antimoniferous sulphide fluids. A subsequent remobilization phase, linked to a late-Hercynian tectonic reactivation, allowed the local redistribution of Sb-Pb associations under the effect of the circulation of oxidizing fluids. This evolution led to the formation of secondary alteration minerals, including bindheimite ($Pb_2Sb_2O_6(O,OH)$), valentinite (Sb_2O_3) and/or senarmontite (Sb_2O_3) and anglesite (PbSO4), reflecting more oxidative conditions and transformation dynamics of the initial sulphide phases (see **Figure 9**). Thirdly, during the Atlas orogeny, supergene alteration processes affected the previous mineralizations. Under the effect of bicarbonate solution circulations, in the context of a wetter climate, a spatial dissociation of the elements Sb, Pb and S occurred, accompanied by the dissolution of galena (PbS) and the secondary precipitation of cerussite ($PbCO_3$) and smithsonite (ZnCO3) within the host carbonate formations. This late phase is characteristic of a shallow subaerial oxidation environment, where geochemical conditions favored the transformation of primary sulphides into secondary carbonates. This integrative framework, combining geochemical, structural, and geodynamic data, highlights the complexity of Sb-Au-Pb-Zn mineraliza-

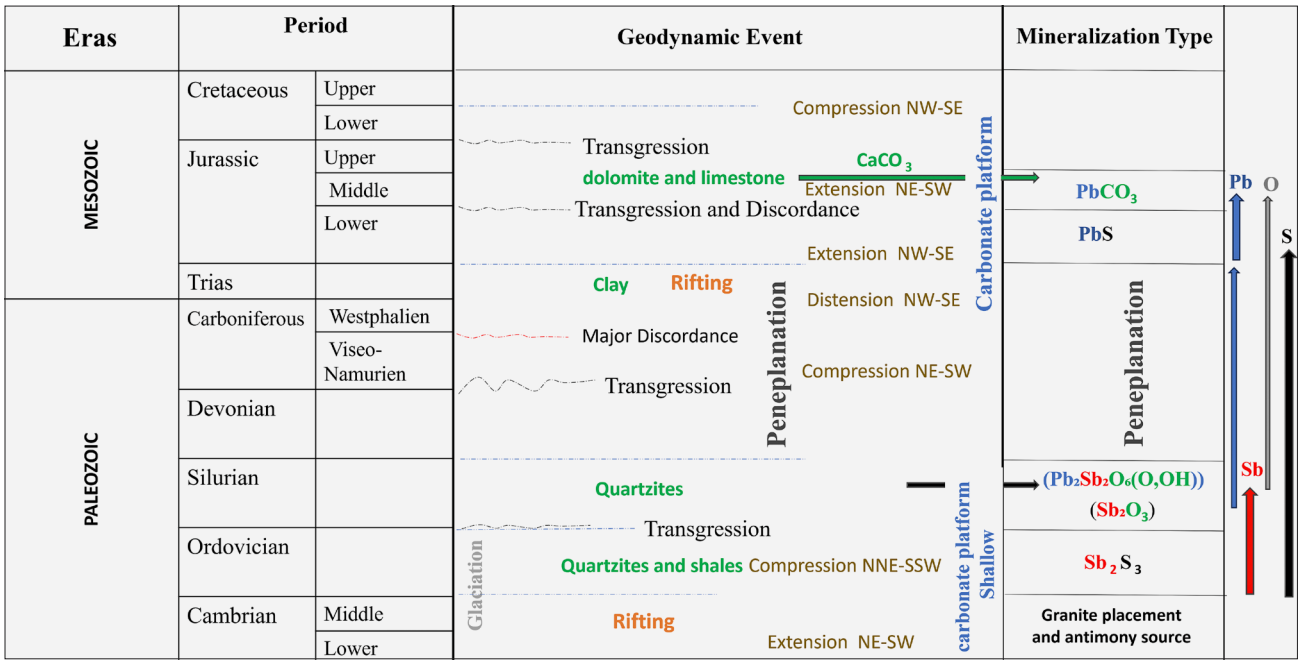

Figure 9. Conceptual model illustrating the paragenetic evolution of the Jbel Houanite mineralization (Sb-Au; Pb-Zn).

tion's in the High Eastern Atlas and underscores the fundamental role of tectonic inheritance and structural reactivation in the genesis and localization of these deposits.

Funding

The authors declare that they have received no funding.

6. References

Adil, S., Bouabdellah, M., Grandia, F., Cardellach, E., & Canals, À. (2004). Geochemistry of fluids associated to the Bou-Dahar Pb-Zn Mississippi Valley-type deposits (Morocco). *Comptes Rendus-Geoscience*, *336*(14), 1265–1272. https://doi.org/10.1016/j.crte.2004.06.010

Ait Ali, A., Choukrad, J., Ouahzizi, Y., Charroud, M., Si Mhamdi, H., Saoud, N., Mounir, S., & Mechaqrane, A. (2025). Integrated remote sensing and field data for lithological mapping and calcite exploration in the Middle Atlas, Morocco. *Scientific African*, *27*, e02521. https://doi.org/10.1016/j.sciaf.2024.e02521

Ait Ali, A., Mohammed, C., Choukrad, J., Ouahzizi, Y., Si Mhamdi, H., Saoud, N., nacer, E., & Mechaqrane, A. (2024). Identification, Characterization, and Deposit Model of Calcite Mineralization in the Middle Atlas Belts, Morocco. *Geosciences*, *14*. https://doi.org/10.3390/geosciences14060154

Ashley, P., & Craw, D. (2004). Structural controls on hydrothermal alteration and gold–antimony mineralisation in the Hillgrove area, NSW, Australia. *Mineralium Deposita*, *39*(2), 223–239.

Azza, A., Abdellah, B., & Moukadiri, A. (2019). Gold and Antimony Mineralizations of Jbel Haouanite (High Atlas, Morocco) in Their Geodynamic Context. *European Scientific Journal*, *15*, 1857–7881. https://doi.org/10.19044/esj.2019.v15n18p336

Bezar, B. S., de Lamotte, D. F., Morel, J. L., & Mercier, E. (1998). Kinematics of large scale tip line folds from the High Atlas thrust belt, Morocco. *Journal of Structural Geology*, *20*(8), 999–1011. https://doi.org/10.1016/S0191-8141(98)00031-5

Blomeier, D. P., & Reijmer, J. J. (2002). Facies architecture of an Early Jurassic carbonate platform slope (Jbel Bou Dahar, High Atlas, Morocco). *Journal of Sedimentary Research*, *72*(4), 462–475.

Bril, H., Bonhomme, M., Marcoux, E., & Baubron, J. (1991). Ages K/Ar des minéralisations de Brioude-Massiac (W-Au-As-Sb; Pb-Zn), Pontgibaud (Pb-Ag; Sn), et Labessette (As-Pb-Sb-Au): Place de ces districts dans l'évolution géotectonique du Massif central français. *Mineralium Deposita*, *26*(3), 189–198.

Caddick, M. J., & Thompson, A. B. (2008). Quantifying the tectono-metamorphic evolution of pelitic rocks from a wide range of tectonic settings: Mineral compositions in equilibrium. *Contributions to Mineralogy and Petrology*, *156*(2), 177–195.

Chapman, R. J., Moles, N. R., Bluemel, B., & Walshaw, R. D. (2022). *Detrital gold as an indicator mineral*. Geological Society Special Publication, 516. pp. 313-336. ISSN 0305-8719.

Charrière, A., Haddoumi, H., & Mojon, P.-O. (2005). Découverte de Jurassique supérieur et d'un niveau marin du Barrémien dans les «couches rouges» continentales du Haut Atlas central marocain: Implications paléogéographiques et structurales. *Comptes Rendus Palevol*, *4*(5), 385–394.

Charroud, M., (2002). Evolution géodynamique des Hauts Plateaux (Maroc) et de leurs bordures du Mesozoique au Cénozoique. *Université de Fes, These d'Etat.–315 Pp, Université de Fes, These d'Etat.–315 pp.*

Charroud, A., Charroud, M., Fedan, B., Laville, E., Rioult, M., Piqué, A., Du Dresnay, R., & Medina, F. (1996). Dynamique sédimentaire des formations triasiques du Moyen Atlas méridional. *Le Permien et Le Trias Du Maroc: État Des Connaissances, PUMAG, Marrakech*, 269–289.

Chellai, E. H., Youbi, N., Bamiki, R. E., Ettaki, M., Ibouh, H., Marzoqi, M., & Ait-Bihi, A. (2024). Evolution of the Atlasic Domain During the Alpine Cycle in the Broader Sense: General Outline of the Evolution of the Tethys. In *The Geology of North Africa* (pp. 187–220). Springer.

Choukrad, J. (2022). *Geological context of the emplacement of mineralizations in the Eastern High Atlas* [Doctorat]. Sidi Mohamed Ben Abdellah University.

Choukrad, J., Abdelkhiar, A. ali, Youssef, O., & Mohammed, C. (2022). Geology, Mineralogy, Geochemistry and deposit model of Iron and Manganese in Bouarfa mine, Eastern High Atlas, Morocco. *Scientific African*, e01401. https://doi.org/10.1016/j.sciaf.2022.e01401

Choukrad, J., Ali, A., Mhamdi, H. S., Ouahzizi, Y., El Moutaouakkil, N., & Charroud, M. (2023). Contribution of Landsat 8 OLI imagery to mapping of lithological series and lineaments: Implications for Pb-Zn mineralization exploration in the Boudahar Massif, Eastern High Atlas, Morocco. *Estudios Geológicos*, *79*(2), e159–e159.

Choukrad, J., Charroud, M., Mhamdi, H. S., Moutaouakkil, N. E., & Ali, A. A. (2024). Geodynamic, metallographic and geochemical characteristics of the Jbel Klakh copper deposit, Eastern High Atlas, Morocco. *Mining of Mineral Deposits*, *18*(4), 18–25. https://doi.org/10.33271/mining18.04.018

Chovan, M., Hurai, V., Sachan, H., & Kantor, J. (1995). Origin of the fluids associated with granodiorite-hosted, Sb-As-Au-W mineralisation at Dúbrava (Nízke Tatry Mts, Western Carpathians). *Mineralium Deposita*, *30*(1), 48–54.

Clayton, R., & Spiro, B. (2000). Sulphur, carbon and oxygen isotope studies of early Variscan mineralisation and Pb-Sb vein deposits in the Cornubian orefield: Implications for the scale of fluid movements during Variscan deformation. *Mineralium Deposita*, *35*(4), 315–331.

Craw, D., Wilson, N., & Ashley, P. (2004). Geochemical controls on the environmental mobility of Sb and As at mesothermal antimony and gold deposits. *Applied Earth Science*, *113*(1), 3–10.

Delvaux, D., & Sperner, B. (2003). New aspects of tectonic stress inversion with reference to the TENSOR program. *Geological Society, London, Special Publications*, *212*(1), 75–100.

Dill, H. (1998). Evolution of Sb mineralisation in modern fold belts: A comparison of the Sb mineralisation in the Central Andes (Bolivia) and the Western Carpathians (Slovakia). *Mineralium Deposita*, *33*(4), 359–378.

Ece, Ö. I., & Ercan, H. Ü. (2024). Global occurrence, geology and characteristics of hydrothermal-origin kaolin deposits. *Minerals*, *14*(4), 353.

El Hakour, A. (2005). Evaluation des ressources de J. Malek à fin décembre 2005, bordure Sud de la boutonnière de Tamlalt (Haut-Atlas oriental). *Unpublished Report (ONHYM)*, 15.

El Kochri, A. (1996). Géométrie et mécanismes de la déformation du Haut Atlas Centro-oriental (Maroc). *These Doctorat d'Etat, Univ. Med. V, Rabat*.

El Kochri, A., & Chorowicz, J. (1988). Tectonique synsedimentaire et style ejectif dans la couverture mesozoique du Haut Atlas oriental (Maroc); exemple de la boutonniere de Mougueur. *Bulletin de La Société Géologique de France*, *4*(4), 541–550.

El Kochri, A., & Chorowicz, J. (1996). Oblique extension in the Jurassic trough of the Central and Eastern High Atlas (Morocco). *Canadian Journal of Earth Sciences*, *33*, 84–92. https://doi.org/10.1139/e96-009

Faure, M., Mézème, E. B., Duguet, M., Cartier, C., & Talbot, J.-Y. (2005). Paleozoic tectonic evolution of medio-Europa from the example of the French Massif Central and Massif Armoricain. *Journal of the Virtual Explorer*, *19*(5), 1–25.

Haddoumi, H., Aiméras, Y., Bodergat, A.-M., Charrière, A., Mangold, C., & Benshili, K. (1998). Âges et environnements des Couches rouges d'Anoual (Jurassique moyen et Crétacé inférieur, Haut-Atlas oriental, Maroc). *Comptes Rendus de l'Académie Des Sciences-Series IIA-Earth and Planetary Science*, *327*(2), 127–133.

Haddoumi, H., Charrière, A., Andreu, B., & Mojon, P.-O. (2008). Les dépôts continentaux du Jurassique moyen au Crétacé inférieur dans le Haut Atlas oriental (Maroc): Paléoenvironnements successifs et signification paléogéographique. *Carnets de Géologie/Notebooks on Geology*, *A06*, 1–29.

Houari. (2003). *Etude structurale de la boutonnière paléozoïque de Tamlet (Haut Atlas oriental): Sa place dans la chaîne hercynienne du Maroc*.

Houari, M.-R., & Hoepffner, C. (2003). Late Carboniferous dextral wrench-dominated transpression along the North African craton margin (Eastern High-Atlas, Morocco). *Journal of African Earth Sciences*, *37*(1–2), 11–24. https://doi.org/10.1016/S0899-5362(03)00085-X

Iancu, V., Berza, T., Seghedi, A., Gheuca, I., & Hann, H.-P. (2005). Alpine polyphase tectono-metamorphic evolution of the South Carpathians: A new overview. *Tectonophysics*, *410*(1–4), 337–365.

Jacobshagen, V., Brede, R., Hauptmann, M., Heinitz, W., & Zylka, R. (2005). Structure and post-Palaeozoic evolution of the central High Atlas. In *The atlas system of Morocco: Studies on its geodynamic evolution* (pp. 245–271). Springer.

Jaouad, C., Mohammed, C., Nacir, E. M., Naoufal, S., Abdelkhiar, A. A., & Youssef, O. (2024). Geology, Mineralogy and Analysis of Tectonic Fracturing of Barite Mineralization's in Bateun Jeudari Paleozoic basement, Eastern High Atlas, Morocco. *Iraqi Geological Journal*, *57*(1D), 46–59. https://doi.org/10.46717/igj.57.1D.5ms-2024-4-15

Kaoukaya, A., Laadila, M., Fedan, B., & Saadi, Z. (2001). La plate-forme carbonatée liasique au NE d'Errachidia (Haut-Atlas oriental, Maroc): Modèle d'organisation des dépôts margino-littoraux. *Bulletin de l'Institut Des Sciences, Rabat*, *23*, 27–38.

Lafforgue, L., Dekoninck, A., Barbarand, J., Brigaud, B., Bouabdellah, M., Verhaert, M., Mouttaqi, A., & Yans, J. (2021). Geological and geochemical constrains on the genesis of the sedimentary-hosted Bou Arfa Mn(-Fe) deposit (Eastern High Atlas, Morocco). *Ore Geology Reviews*, *133*, 104094. https://doi.org/10.1016/j.oregeorev.2021.104094

Laville, E., Pique, A., Amrhar, M., & Charroud, M. (2004). A restatement of the Mesozoic Atlasic Rifting (Morocco). *Journal of African Earth Sciences*, *38*(2), 145–153. https://doi.org/10.1016/j.jafrearsci.2003.12.003

Leach, D. L., Sangster, D. F., Kelley, K. D., Large, R. R., Garven, G., Allen, C. R., Gutzmer, J., & Walters, S. (2005). *Sediment-hosted lead-zinc deposits: A global perspective*. Economic geology: One hundredth anniversary volume. 561-608. https://doi.org/10.5382/AV100.18

Marcoux, E., & Bril, H. (1986). Héritage et sources des métaux d'après la géochimie isotopique du plomb: Exemple des minéralisations filoniennes (Sb, Pb, Ba, F) du Haut-Allier (Massif Central, France). *Mineralium Deposita*, *21*(1), 35–43.

Mattauer, M., Proust, F., & Etchecopar, A. (1977). Lineation» a» et mecanisme de cisaillement simple lie au chevauchement de la nappe des schistes lustres en Corse. *Bulletin de La Société Géologique de France*, *7*(4), 841–847. https://doi.org/10.2113/gssgfbull.S7-XIX.4.841

Merino-Tomé, Ó., Porta, G. D., Kenter, J. A., Verwer, K., Harris, P., Adams, E. W., Playton, T., & Corrochano, D. (2012). Sequence development in an isolated carbonate platform (Lower Jurassic, Djebel Bou Dahar, High Atlas, Morocco): Influence of tectonics, eustacy and carbonate production. *Sedimentology*, *59*(1), 118–155.

Munoz, M., & Moëlo, Y. (1982). Etude paragénétique de la minéralisation sulfurée complexe (Sb-Pb-Zn...) de Bournac (Hérault, France). *Bulletin de Minéralogie*, *105*(6), 625–632.

Nouayti, A., Khattach, D., Nouayti, N., El Moudnib, L., Hilali, M., & Saadi, O. (2023). Structural modeling of the Paleozoic basement and hydrogeological study: Contribution of geology and aeromagnetic data of the Eastern High Atlas (Morocco). *Modeling Earth Systems and Environment*, *9*(1), 1199–1213.

Oh, C. W., Kim, S. W., Ryu, I., Okada, T., Hyodo, H., & Itaya, T. (2004). Tectono-metamorphic evolution of the Okcheon metamorphic belt, South Korea: Tectonic implications in East Asia. *Island Arc*, *13*(2), 387–402.

Piqué, A., & Michard, A. (1989). Moroccan Hercynides: A synopsis. The Paleozoic sedimentary and tectonic evolution at the northern margin of West Africa. *American Journal of Science*, *289*, 286–330. https://doi.org/10.2475/ajs.289.3.286

Rajeshkumar, R., Vignesh, S., Singh, L. K., & Srinivasan, A. (2024). Development of Mg-Sb-Sn and Mg-Sb-Ca Magnesium Alloys for Automotive Applications: Microstructure, Mechanical Properties, and Corrosion Behavior Analysis. *Journal of Materials Engineering and Performance*. https://doi.org/10.1007/s11665-024-09539-8

Sun, X., Li, R.-Y., Sun, H.-Y., Olin, P. H., Santosh, M., Fu, B., & Deng, J. (2024). Genesis of Pb–Zn-Ag-Sb mineralization in the Tethys Himalaya, China: Early magmatic-hydrothermal Pb–Zn(-Ag) mineralization overprinted by Sb-rich fluids. *Mineralium Deposita*, *59*(7), 1275–1293. https://doi.org/10.1007/s00126-024-01264-5

Talih, A., Aboussalam, Z., Becker, R., Saadi, M., & Benmlih, A. (2022). Stratigraphy and tectono-sedimentary processes of allochthonous and autochthonous Devonian deposits of the Tisdafine Basin, Eastern Anti-Atlas, Morocco. *Morocco Bulletin De L'institut Scientifique*, *44*(October), 43–69.

Verhaert, M., Bernard, A., Dekoninck, A., Lafforgue, L., Saddiqi, O., & Yans, J. (2017). Mineralogical and geochemical characterization of supergene Cu–Pb–Zn–V ores in the Oriental High Atlas, Morocco. *Mineralium Deposita*, *52*(7), 1049–1068. https://doi.org/10.1007/s00126-017-0753-5

Verwer, K., Merino-Tomé, O., Kenter, J. A., & Della Porta, G. (2009). Evolution of a high-relief carbonate platform slope using 3D digital outcrop models: Lower Jurassic Djebel Bou Dahar, High Atlas, Morocco. *Journal of Sedimentary Research*, *79*(6), 416–439.

Wei, H., Xiao, K., Shao, Y., Kong, H., Zhang, S., Wang, K., Li, Q., Chen, B., Xiang, J., & Wen, C. (2020). Modeling-based mineral system approach to prospectivity mapping of stratabound hydrothermal deposits: A case study of MVT Pb-Zn deposits in the Huayuan area, northwestern Hunan province, China. *Ore Geology Reviews*, *120*, 103368. https://doi.org/10.1016/j.oregeorev.2020.103368

SAŽETAK

Geodinamička i paragenetska evolucija mineralizacije Jbel Houanit (Sb-Au; Pb-Zn) u istočnome Visokom Atlasu, Maroko

Jbel Houanite važna je metalogenetska regija bogata polimetalnom mineralizacijom (Sb-Au-Pb-Zn-Ba-Fe-Cu) smještena u sjevernome dijelu istočnoga Visokog Atlasa u Maroku, uz sjeverni rasjed Visokoga Atlasa. Najranija identificirana mineralizacija odgovara kvarcnim žilama koje su bogate antimonom i zlatom te se nalaze u paleozojskim formacijama, dok kasnija mineralizacija odgovara Pb-Zn naslagama u lijaskim vapnencima. Geološkim rekognosciranjem i istraživanjem minerala u regiji Jbel Houanite utvrđena je prisutnost mineralizacije antimona u obliku stibnita (Sb_2S_3) i bindheimita ($Pb_2Sb_2O_6(O,OH)$), dok se olovna mineralizacija u sedimentnome pokrovu sastoji od galenita (PbS) i cerusita ($PbCO_3$). Anomalije olova blisko su vezane uz prisutnost antimona te je ova mineralizacija rezultat hidrotermalne remobilizacije tijekom faza Atlasa koje su reaktivirale rasjede u stijenama podine, olakšavajući nastanak mineralizacije olova u sklopu sustava tipa Mississippi Valley (MVT). Petrografska i geokemijska istraživanja mineralnih parageneza omogućila su uspostavljanje vremenskih odnosa između događaja mineralizacije: primarna Sb-Au mineralizacija povezana je s kasnohercinskom ekstenzijskom tektonikom, dok je Pb-Zn mineralizacija povezana s ranim atlaskim kompresijskim fazama. Ova sekvencijska evolucija upućuje na složenu polifaznu tektono-metalogenetsku povijest koja je kontrolirala nastanak orudnjenja. Rezultati ovih istraživanja doprinose boljem razumijevanju genetskih modela Sb-Au-Pb-Zn mineralizacije u istočnome Visokom Atlasu te pokazuju ključnu ulogu tektonike i strukturne reaktivacije u stvaranju i lokalizaciji orudnjenja.

Ključne riječi:
antimon, olovo, paragenetska evolucija, paleozojska podloga, mezokenozojski pokrov, istočni Visoki Atlas, Maroko

Author's contribution

Jaouad Choukrad (PhD Thesis in Mining and structural Geology): conceptualization, investigation, conceptualization, data curation, formal analysis, funding acquisition and software. **Ait Ali Abdelkhiar** (PhD Thesis in Economic Geology): conceptualization, investigation, conceptualization. **Mohammed Charroud** (Full Professor): supervision, validation, visualization, writing – original draft and writing – review & editing. **Nacir El moutaouakkil** (Professor): investigation, methodology, project administration. **Boubker Boukili** (Professor): investigation, software, investigation, methodology, and project administration, **Amine Talih** (PhD Thesis in Stratigraphy and Paleontology): resources, software.
All authors have read and agreed to the published version of the manuscript.